Desalination and Water Treatment
www.deswater.com

1944-3994/1944-3986 © 2012 Desalination Publications. All rights reserved
doi: 10.1080/19443994.2012.677513

46 (2012) 188–195
August

Taylor & Francis
Taylor & Francis Group

A comparative study of the photocatalytic efficiency of Degussa P25, Qualigens, and Hombikat UV-100 in the degradation kinetic of congo red dye

Suhas R. Patil[a,c,d,*,1], U.G. Akpan[c,e], B.H. Hameed[c], S.K. Samdarshi[a,b,2]

[a]*School of Physical Sciences, North Maharashtra University, P.B. No. 80, Jalgaon, Maharashtra, India*
Fax: +91 257 2235642; email: suhaspatil55@yahoo.co.in
[b]*Department of Energy, Solar & Energy Materials Laboratory, Tezpur University, Tezpur, Assam 784028, India*
[c]*School of Chemical Engineering, Engineering Campus, Universiti Sains Malaysia, Nibong Tebal, Penang 14300, Malaysia*
[d]*Department of Physics, Dr. Annasaheb G.D. Bendale Mahila Mahavidyalaya, Jalgaon, Maharashtra 425 001, India*
[e]*Chemical Engineering Department, Federal University of Technology, P.M.B. 65, Minna, Nigeria*

Received 18 September 2011; Accepted 30 January 2012

ABSTRACT

The photocatalytic efficiency of three TiO_2 photocatalysts; Degussa P25, Qualigens, and Hombikat UV 100 has been investigated on the degradation kinetic of congo red dye. The crystal phases, structures, and crystallite sizes of the catalysts were analyzed by X-ray diffraction, microstructure, and morphology by transmission electron microscopy, and surface area and pore-size distributions by nitrogen physisorption. The results of the kinetic study revealed that the activities of the photocatalysts were dependent on their particle sizes, and the best activity was obtained with Hombikat UV-100, which was of the smallest particle size, was mesoporous, and had the largest surface area. The activation energy required for the degradation of the congo red dye was found to increase proportionately with the particle size of the catalysts. The effects of various operational parameters such as catalysts dosages, initial dye concentration, and temperature were systematically studied in order to achieve maximum degradation efficiency. The results of the investigations suggest that Hombikat, another model photocatalyst, can be used more effectively in the place of Degussa P25 in photocatalytic degradation of congo red dye.

Keywords: Congo red dye; Photocatalyts; Photocatalysis; Adsorption; Dye removal; Dye degradation

1. Introduction

Wastewaters generated by the textile industries contain considerable amount of nonfixed dyes, especially azo dyes, and a huge amount of inorganic salts that represent an increasing environmental danger. Azo dyes with aromatic moieties linked together by azo (–N=N–) chromophores represent the largest class of dyes used in textile, processing, and other industries. Approximately 50–70% of the dyes are aromatic azo compounds [1,2]. It is well known that some azo dyes are highly carcinogenic [3,4], and hence must be removed from the wastewater before being discharged.

---

[1] Present address: Department of Physics, Dr. Annasaheb G.D. Bendale Mahila Mahavidyalaya, Jalgaon-425 001, Maharashtra, India.

[2] Present address: Solar & Energy Materials Laboratory, Department of Energy, Tezpur University, Tezpur, Assam 784028, India.

*Corresponding author.

Much effort has been made to remove these substances from wastewaters before discharge into water channels. Such methods as traditional physical techniques: adsorption by activated carbon/other adsorbents, biological treatments, etc proved to be inadequate for the treatment of wastewaters containing azo dyes [5,6]. This has diverted the focus from these methods to a newly emerging technique, photocatalysis [7–9], as the latter brings about a complete mineralization of the target pollutant [10,11]. Many semiconductor photocatalysts [12–15] have been employed in the photocatalytic degradation of various pollutants, but TiO_2-based photocatalysts enjoyed a wider application [16,17] possibly because of some advantages such photocatalysts have over others [18].

Titanium dioxide has two important crystalline phases (anatase and rutile) and an amorphous phase (brokite). The pure anatase and rutile have band gap energies of 3.2 and 3.0 eV, respectively [19], which are very important parameters that regulate their photocatalytic potentialities. Pure anatase and mixed (anatase + rutile) phases have been reported to show high photocatalytic activity [20,21]. Various commercial TiO_2 photocatalysts with different sizes, surface area, and crystalline phases/phase compositions are available in the market. The list includes but is not limited to Degussa P25, Hombikat UV-100, Qualigens, PC500, TiO_2-Sigma product, anatase TiO_2-British Drog House. It is noted with interest that many works have been reported on the effectiveness of Degussa P25 in photocatalytic processes [22,23] and doping/compositing [24,25] to make it more active in environmental decontamination. The activity of catalyst varies from pollutant to pollutant. Similarly, the degradation of a particular pollutant varies with catalysts. However, particle size of the catalyst is an important parameter in the photocatalytic process, since it has a direct effect on the surface area of the catalyst. With a smaller particle size, the number of active surface sites increases, and so does the surface charge carrier transfer rate in photocatalytic processes. Earlier published results [22,34] indicated a decrease in the activation energy with increase in particle sizes of the catalysts. The trend that may be expected here is an increase in the difficulties of a reaction to start up with increase in particle sizes of the catalysts. This will therefore mean an increase in the activation energy with increase in particle sizes of the catalysts. This present work was therefore designed to study the photocatalytic activities of three commercially available TiO_2, Degussa P25, Hombikat UV 100, and Qualigens (which are of different particle sizes); compare their activities vis-à-vis their particle sizes and proffer recommendations as to why some other photocatalysts other than Degussa P25 could be considered for compositing in photocatalytic reactions. It is the intention of this study to also verify the effects of particle size on the activation energy required for the photocatalytic degradation of congo red (CR) dye.

2. Materials and methods

2.1. Catalyst and organic dye

In the present work, TiO_2 of different types: Degussa P-25 (P-25, International Chemical, India); Qualigens (Qualigens, Fine Chemicals, India); and Hombikat UV-100 (H UV-100, Sachtleben Chemie, Duisburg, Germany) were used as the photocatalyst, while the organic dye, congo red (CR, S.D. Fine-Chemical Ltd., India), was used as a pollutant. Stock solutions of different concentrations (35–175 mg L^{-1}) were prepared with distilled water. All chemicals were used as received without further purification in this study.

2.2. Reactor

Fig. 1 shows the experimental setup of batch-type UV photoreactor. A 125 W medium pressure UV lamp (SAIC, Chennai, India) with a peak at 360 nm was used as a photon energy source. The intensity of UV light radiation was 1.320×10^{-3} W/cm^2 determined by a research radiometer (International light IL-1700, USA) with a UV detector (SED-005 range 200–400 nm).

2.3. Experimental procedure

The stock solution of the organic dye loaded with the catalyst was stirred thoroughly for about 30 min in the dark to establish adsorption–desorption equilibrium. Thereafter, it was irradiated, while the stirring of the slurry was maintained. Samples were drawn from the solution at preset time intervals. The samples were centrifuged at 1,200 rpm (REMI, India) for

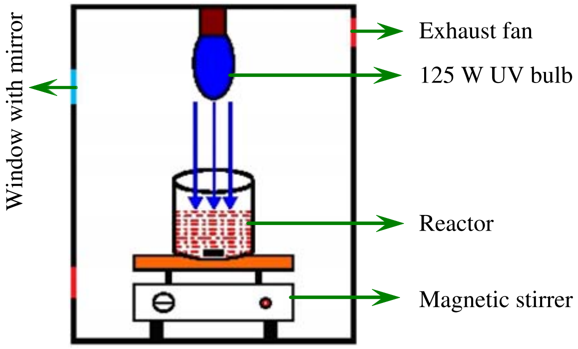

Fig. 1. Experimental setup of a batch-type UV photoreactor.

sufficient time (30 min), and the clear solution was then analyzed using UV–Visible spectrophotometer (UV-1601 Shimadzu, Japan) at CR maximum absorbance, $\lambda_{max} = 498$ nm.

2.4. Characterization

Powder X-ray diffraction (XRD) patterns of the catalysts were measured by D8 Advanced X-ray solution with an α_1 configuration using Cu Kα radiation (1.5,406 Å) in a wide-angle range (2θ) from 20° to 80° with a step size of 0.0342. The average particle size (D_p) was determined from Scherrer's equation using the broadening of the (1 0 1) anatase and (1 1 0) rutile peaks' reflection [17]:

$$D_p = 0.94\lambda/\beta\cos\theta \qquad (1)$$

where λ is the wavelength of X-ray, θ is the diffraction angle, and $\beta_{1/2}$ is full-width at half-maximum (FWHM) of a characteristic diffraction peak. The amount of rutile phase content in Degussa P-25 catalyst sample was estimated using the Spurr equation [26]:

$$F_R = \left(1 + \left(0.884 I_{A(101)}/I_{R(110)}\right)\right)^{-1} \qquad (2)$$

where F_R is the mass fraction of rutile in the sample and $I_{A(101)}$ and $I_{R(110)}$ are the integrated main peak intensities of anatase and rutile, respectively.

Transmission electron microscopy (TEM) was performed using Techni-20 Philips model, operating at 200 kV electron beam, and having 65×10^6 magnification capacity. Nitrogen adsorption–desorption isotherms of catalysts were collected on ASAP 2020 V3.02 H Micromeritics surface area and porosity analyzer at 77 K. The Brunauer–Emmett–Teller (BET) surface area was calculated from the linear part of the BET plot. The pore-size distribution plots were obtained by using the Barret–Joyner–Halenda (BJH) model.

3. Results and discussion

3.1. Characterization of the catalysts

3.1.1. X-ray diffraction

Fig. 2 shows the XRD patterns of the three commercial TiO_2 powders taken at room temperature. The anatase phase characteristic peaks were identified at $2\theta = 25.3°$ (1 0 1), 36.9° (1 0 3), 37.8° (0 0 4), 38.5° (1 1 2), 48.0° (2 0 0), 53.8° (1 0 5), 55.0° (2 1 1) 62.2° (2 1 3), 62.6° (2 0 4), 68.7° (1 1 6), 75.0° (2 1 5), and 76.0° (3 0 1); while the rutile phase characteristic peaks were identified at $2\theta = 27.5°$ (1 1 0), 36.2° (1 0 1), and 41.2° (1 1 4). It is clear from Fig. 2 that H UV-100 and Qualigens exhibited a uniform anatase phase, whereas P-25 is a mixture of anatase and rutile phases. The estimated values of anatase and rutile phases are recorded in Table 1.

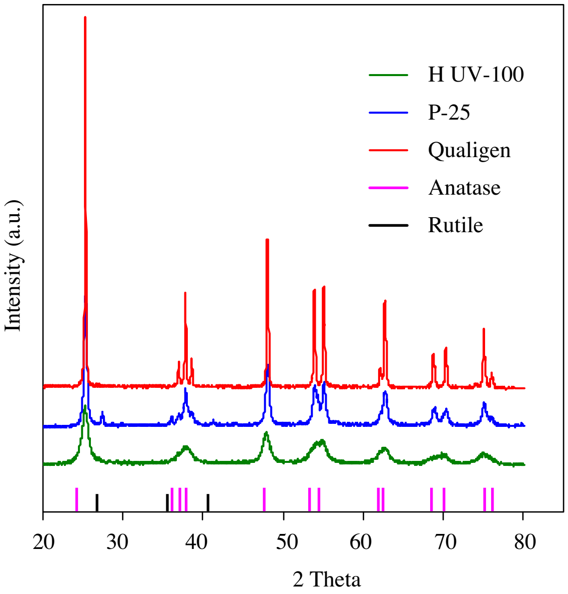

Fig. 2. X-ray diffraction pattern of P-25, Qualigens, and H UV-100 catalysts powder samples.

The FWHM of the reflection is the characteristic of the particle size of the corresponding phase (for anatase (1 0 1) and rutile (1 1 0)). By the results (Table 1), H UV-100 is of the smallest particle size among the understudied photocatalysts, followed by P-25, while Qualigens has the largest size. The XRD results correlate well with the results obtained by the TEM analysis. Since P-25 is anatase and rutile mixed crystals, the percentage of rutile phase present was

Table 1
Properties of the various catalysts employed in the study

TiO_2 catalysts	Particle size by XRD (nm)	Particle size by TEM (nm)	BET surface area ($m^2 g^{-1}$)	Crystal forms
P-25	20.8 (A) and 42.9 (R)	30	52	85% (A) + 15% (R)
Qualigens	55.5	60	13	100% (A)
H UV-100	8.2	⩽10	255	100% (A)

Note: A, anatase phase; R, rutile phase.

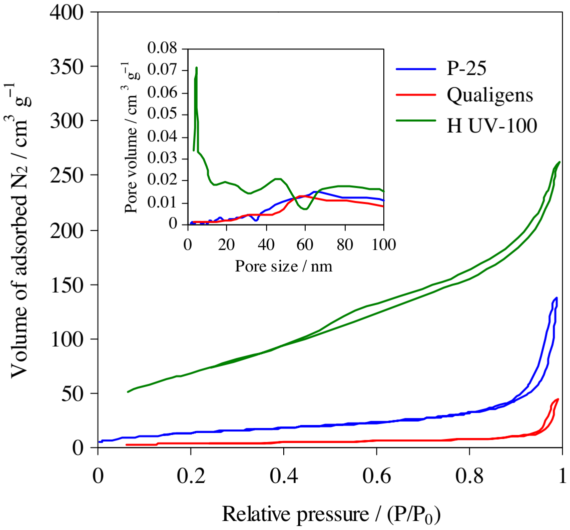

Fig. 3. N_2 adsorption–desorption isotherms and BJH pore-size distribution (inset) of P-25, Qualigens, and H UV-100 catalysts powder samples.

estimated by the Spurr equation to be 15%, while anatase was 85%.

3.1.2. BET surface area

Fig. 3 depicts N_2 adsorption–desorption isotherms for the three commercial TiO_2; P-25, Qualigens, and H UV-100 powders. The adsorption–desorption isotherms of P-25 and Qualigens powders are clearly indicating type II adsorption–desorption isotherms with negligible H_3-type hysteresis loop for the relative pressure P/P_0 in the range of 0.9–1 and 0.95–1, respectively. These are typical characteristics of nonporous or macroporous materials according to the International Union of Pure and Applied Chemistry (IUPAC) classification [27]. Nevertheless, the isotherms of the H UV-100 powder are indicating type IV adsorption–desorption isotherms with long H_3-type hysteresis loops at 0.4–1 relative pressure (P/P_0) range, which are the characteristics of mesosporous materials [22]. Pore-size distributions of the three commercial TiO_2 powder samples were determined using the desorption branch of the nitrogen-desorption isotherms by the BJH model. Fig. 3 (inset) shows pore-size distribution curves of these catalysts. The pore size for H UV-100 is in the range of 2.74–5.26 nm, with a maximal point at 4.26 nm. This range is indicative of a narrow size mesospore. On the other hand, there are no maximal points observed in the case of P-25 and Qualigens. Nevertheless, after 50 nm pore size; there was a slight increase in the pore volume for P-25 and Qualigens powders. The estimated BET surface areas of all the samples are presented in Table 1. The BET surface area of H UV-100 catalyst is $255\,m^2\,g^{-1}$ and this shows that it has a very large surface available for photocatalysis. The surface areas of P-25 ($52\,m^2\,g^{-1}$) and Qualigens ($13\,m^2\,g^{-1}$) are very much smaller than that of H UV-100. This, in addition to good pore-size distribution, is responsible for the high performance of the H UV-100 over other catalysts in the UV light degradation of the CR dye.

3.1.3. Transmission electron microscopy

TEM analysis was performed for each of the commercial TiO_2 samples to confirm their nano-size of particles and the morphological structure of the sample. Fig. 4 shows the TEM images of P-25, Qualigens, and H UV-100. It can be seen that the crystals of all samples are spherical in shape having different nano-size particles. The average particle sizes of P-25 and Qualigens samples are about 30 and 60 nm, respectively, whereas the particle size of H UV-100 is found to be ⩽10 nm, which is in accordance with the particle size evaluated by Scherrer's formula. Small particle size results typically result in an enhanced surface area, TEM and XRD results thus confirming the BET measurements.

3.2. Adsorption, photolysis, and photocatalytic study

In the preliminary experiment, adsorption and photolysis were performed on the CR dye using the commercial TiO_2 P-25, Qualigens, and H UV-100. This

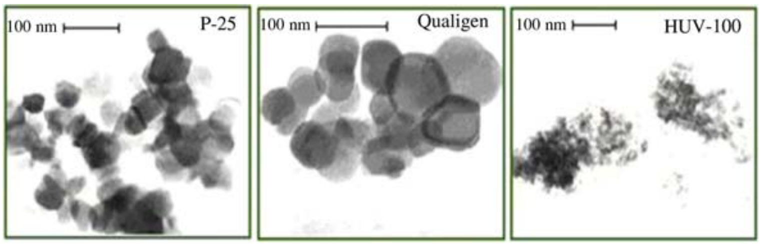

Fig. 4. TEM images of P-25, Qualigens and H UV-100 TiO_2 catalyst powder.

was done to study the effects of each or a combination of these processes on the photocatalytic degradation of CR dye. During the initial dark periods (lamp off) indicated by a negative time scale, it takes 30 min to establish the adsorption–desorption equilibrium (Fig. 5). As it can be seen in Fig. 5, the adsorption properties of different commercial powders were different. In the case of H UV-100, nearly 23% of the available CR dye was adsorbed, while in the case of P-25 and Qualigens only 11 and 9% were adsorbed, respectively. The high adsorption capacity of H UV-100 correlates well with its surface morphology, particle size, and high surface area. There was no evidence of the CR dye removal in the dark experiment carried out without photocatalyst. These results indicate that the adsorption of CR dye on the catalysts surface increases with increasing surface area of the catalyst.

Direct photolysis of the CR dye was also checked under the adopted UV irradiation conditions, in the absence of catalysts. It is observed that the CR dye can be slightly removed by direct photolysis, but at a significantly lower rate compared to the photocatalytic process. From Fig. 5, it can be seen that photocatalytic degradation of CR dye is significantly faster in the presence of H UV-100 (97% within 25 min) than P-25 (85%) and Qualigens (80%) after 60 min. The faster degradation of CR dye in the presence of H UV-100 could be attributed to its large surface area and smaller crystallite size. It must be noted that the photocatalytic process occurs as the pollutant is adsorbed on the surface of the catalyst; hence, a catalyst with high adsorptivity is expected to favor the photocatalytic degradation.

A similar effect of the crystal size and crystal phase on the degradation of 4-chloronitrobenzene under UV light irradiation was observed for hydrothermally synthesized TiO_2 hollow microspheres and P-25 [28]. Smaller particle sizes are usually associated with higher surface areas, which could be the influential factor in photocatalytic degradation reactions because a large contact surface exposed to organic pollutant molecules promotes the reaction rate [29,30]. A titania particle size of around 10 nm has been suggested to produce the highest photocatalytic oxidation rates [31].

3.3. Effect of catalyst loading

A set of experiments in which the weight of catalysts used was varied was carried out to determine the effect of catalyst loading on the rate constant (*k*) of degradation of CR dye. The rate constant, *k*, was plotted against the amount of catalyst (Fig. 6). All types of catalysts exhibited a similar trend, there was a steady increase in the degradation rate constant (*k*) of CR dye up to 300 mg L^{-1}. Any further increase in the amount of catalyst beyond 300 mg L^{-1} was detrimental to the process. At higher catalyst loading, the photon energy is screened by the excess catalyst and hence the rate of degradation is reduced. Furthermore, at higher catalyst loading, it is difficult to maintain the homogene-

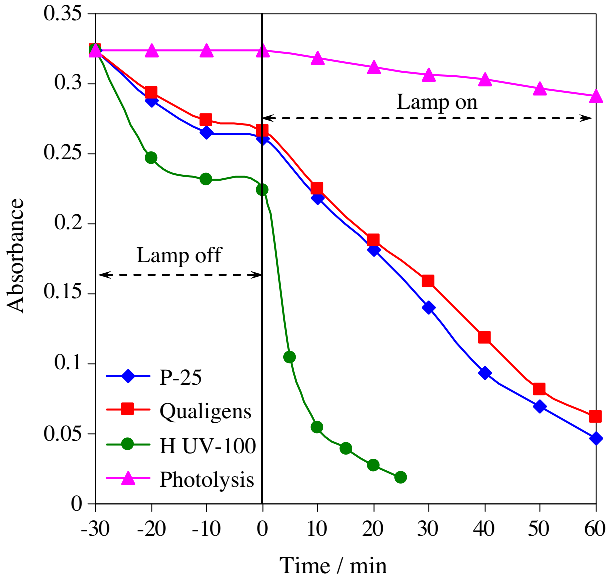

Fig. 5. Comparison of the photocatalytic efficiency of the commercial photocatalysts in the degradation of the CR dye. Reaction conditions: dye concentration, 70 mg L^{-1}; catalyst loading, 300 mg L^{-1}; reaction temperature, 308 K.

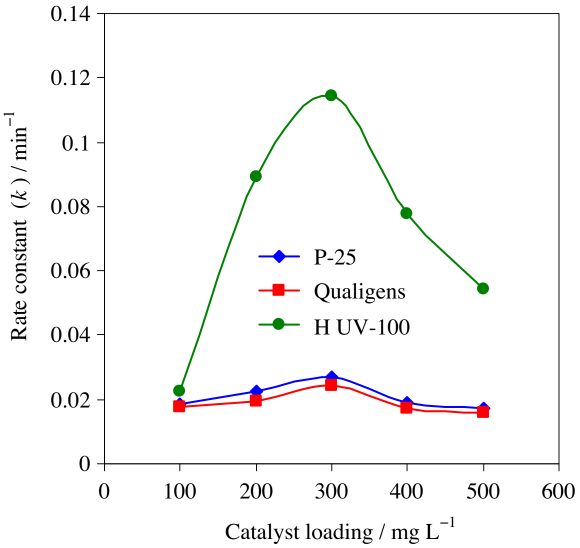

Fig. 6. Effect of catalyst loading on the degradation rate constant (*k*) of the CR dye. Reaction conditions: CR dye concentration, 70 mg L^{-1}; reaction temperature, 308 K.

ity of the suspension due to particle agglomeration, which decreases the number of active sites [32]. The results presented in Fig. 6 revealed that the maximum degradation rate for this system was attained at 300 mg L^{-1} catalyst loading in the case of all catalysts. Nevertheless, H UV-100 demonstrated superiority in its degradation ability in comparison with the P-25 and Qualigens for the CR dye. These results are indicative of the fact that the rate constant (*k*) increases with increase in the catalyst surface area.c

3.4. Effect of initial dye concentration

The effect of initial dye concentrations on the degradation rate of CR dye was studied by varying the dye concentration from 35 to 140 mg L^{-1} with constant catalyst loading and the results are shown in Fig. 7. All types of catalysts exhibited a similar trend. There is a linear decrease in the degradation rate constant (*k*) of CR dye up to 105 mg L^{-1} of the CR dye concentration, followed by a slow reduction to a constant. These results indicate that at high CR dye concentration, the high color intensity of the dye reduces the intensity of the photon energy reaching the catalyst, and as such reduced the rate of the degradation of the CR dye [6]. The results, Fig. 7, revealed that H UV-100 showed a better performance in the degradation of CR dye at all initial concentrations than both P-25 and Qualigens. A similar trend has been reported for the photocatalytic oxidation of bromophenol blue (concentration range from 5 to 40 mg L^{-1}) under UV irradiation at 365 nm for P25 and PC500-Millennium catalysts [22] and decolorization of methyl orange and rhodamine 6G (concentration range from 5 to 100 mg L^{-1}) under solar irradiation [33].

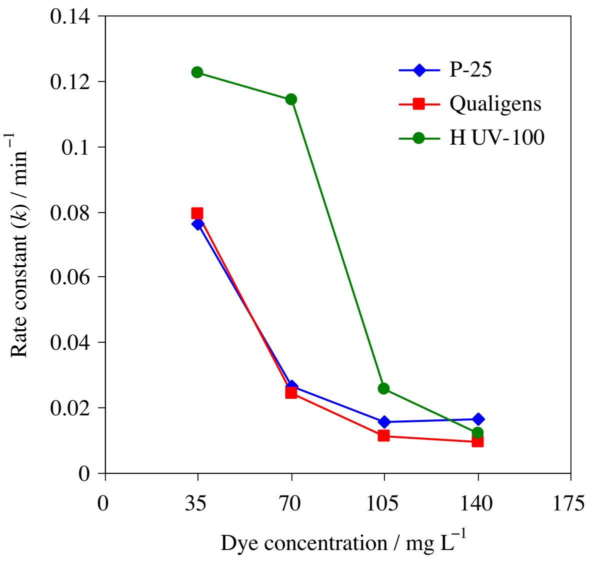

Fig. 7. Effect of initial dye concentrations on the degradation rate constant (*k*) of the CR dye. Reaction conditions: catalyst loading, 300 mg L^{-1}; reaction temperature, 308 K.

3.5. Effect of temperature

A separate study was conducted to evaluate the activation energy required for the degradation of CR dye using P-25, Qualigens, and H UV-100 photocatalysts. Other parameters (dye concentration and catalysts loading) were kept constant, while the temperature of the colloidal solution was varied. Fig. 8 shows the effect of colloidal solution temperature (varying from 278 to 335 K) on degradation rate constant (*k*) of CR dye. The results, Fig. 8, showed that the degradation rate constant of CR dye increased rapidly with increase in temperature when H UV-100 was used as a photocatalyst, but P-25 and Qualigens showed a slight increase in the degradation rate constant of CR dye as the temperature of the colloidal solution increased. Recently, similar effect of temperature (from 283 to 323 K) on photocatalytic degradation of bromophenol blue with P25 and PC500-Millennium catalysts had been reported [22].

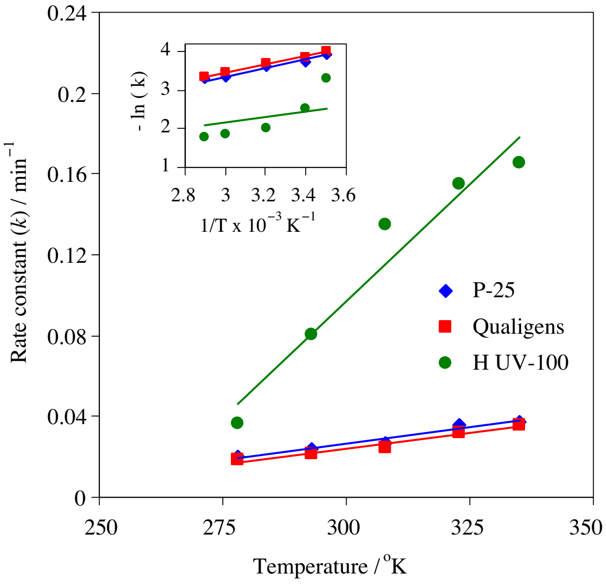

Fig. 8. Effect of temperature on degradation rate constant (*k*) and Arrhenius plot (inset) for the photoreaction of the CR dye. Reaction conditions: catalyst loading, 200 mg L^{-1}; CR dye concentration 70 mg L^{-1}.

The activation energy for the degradation of CR dye by the various photocatalysts was evaluated and a comparison was made based on each photocatalyst particle size. The results, Fig. 8 (inset), shows the Arrhenius

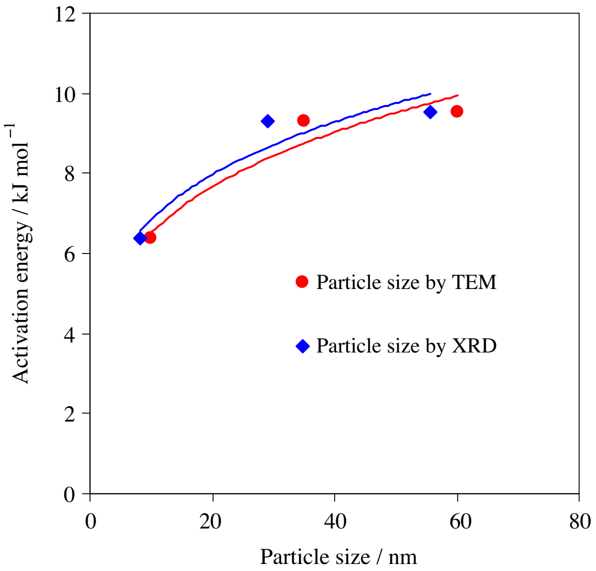

Fig. 9. Effect of particle sizes of the catalyst on the activation energy for the degradation of the CR dye.

plot for the photoreaction. The values of the activation energy obtained from Fig. 8 (inset) are 6.39, 9.29 and 9.52 kJ mol^{-1} for H UV-100, P-25, and Qualigens, respectively. It is well known that activation energy for any reaction is the energy necessary to activate the reaction. It was therefore expedient to correlate this energy with the particle sizes of the catalysts available. Hence, Fig. 9 presents the effect of particle sizes of the catalyst on the activation energy for the degradation of CR dye. Since the catalyst with the smallest particle sizes (H UV-100) showed a higher degradation rate for the CR dye (Fig. 7), it is also expected that a minimum energy will be required for its activation than for the others. The results, Fig. 9, are in conformity with this expected trend. It takes less energy (6.39 kJ mol^{-1}) for the catalyst with the smallest particle size (H UV-100) to be activated, while the highest energy of 9.52 kJ mol^{-1} was required to activate the same reaction with a catalyst that has the biggest particle size (Qualigens). Previous reports [22,34] are inconsistent with the results of the present study. The two previous literatures showed a decrease in activation energy with increase in particle sizes. It must therefore be noted and emphasized that activation energy is supposed to increase with the size of the catalyst particles.

4. Conclusion

The photocatalytic efficiency of three commercially available TiO_2 photocatalysts; Degussa P25, Qualigens, and Hombikat UV-100 have been investigated on the degradation kinetic of congo red dye. The activities of the photocatalysts are controlled by their particle sizes. Qualigens, with the largest particle sizes and least surface area, is less effective in the degradation of congo red dye, while Hombikat UV-100 with the largest surface area and smallest particle sizes is the most effective of all the photocatalysts. Activation energy for the degradation of congo red dye increased with the increase in particle sizes of the catalysts. The optimum catalyst dosage for all catalysts considered is 300 mg L^{-1} and the degradation reaction is more difficult at higher initial concentrations of the dye solution. Both Hombikat UV-100 and Qualigens are made up of 100% anatase phase, while Degussa is a mixture of anatase and rutile phases. In comparison with P-25 and Qualigens, Hombikat UV-100 has been excellent in the degradation of the congo red dye. In future work, surface doping/compositing will be considered to test its ability in this regard.

Acknowledgments

Authors gratefully acknowledge the financial support provided by UGC, New Delhi and CSIR, New Delhi (India) and Universiti Sains Malaysia, Malaysia, for providing Postdoctoral Fellowship.

References

[1] R. Molinari, F. Pirillo, M. Falco, V. Loddo, L. Palmisano, Photocatalytic degradation of dyes by using a membrane reactor, Chem. Eng. Process. 43 (2004) 1103–1114.
[2] S. Bilgi, C. Demir, Identification of photooxidation degradation products of C.I. Reactive Orange 16 dye by gas chromatographye mass spectrometry, Dyes Pigments 66 (2005) 69–76.
[3] H. Lachheb, E. Puzinat, A. Houas, M. Ksibi, E. Elaloui, C. Guillard, J.M. Hermann, Photocatalytic degradation of various types of dyes (alizarins, crocein orange g, methyl red, congo red, methylene blue) in water by UV-irradiatedtitania, Appl. Catal. B: Environ. 39 (2002) 75–90.
[4] F. Kiriakidou, D.I. Kondarides, X.E. Verykios, The effect of operational parameters and TiO_2-doping on the photocatalytic degradation of azo-dyes, Catal. Today 54(1) (1999) 119–130.
[5] I.K. Konstantinou, T.A. Albanis, TiO_2-assisted photocatalytic degradation of azo dyes in aqueous solution: Kinetic and mechanistic investigations—a review, Appl. Catal. B: Environ. 49 (2004) 1–14.
[6] U.G. Akpan, B.H. Hameed, Parameters affecting the photocatalytic degradation of dyes using TiO_2-based photocatalysts: A review, J. Hazard. Mater. 170 (2009) 520–529.
[7] B. Krishnakumar, K. Selvam, R. Velmurugan, M. Swaminathan, Influence of operational parameters on photodegradation of Acid Black 1 with ZnO, Desalin. Water Treat. 24 (2010) 132–139.
[8] A.H. Ali, S. Kapoor, S.K. Kansal, Studies on the photocatalytic decolorization of pararosanilne chloride dye and its simulated dyebath effluent, Desalin. Water Treat. 25 (2011) 268–275.
[9] P. Bansal, N. Bhullar, D. Sud, Studies on photodegradation of malachite green using TiO_2/ZnO photocatalyst, Desalin. Water Treat. 12 (2009) 108–113.
[10] B.H. Hameed, U.G. Akpan, K.P. Wee, Photocatalytic degradation of acid red 1 dye using ZnO catalyst in the presence and absence of silver, Desalin. Water Treat. 27 (2011) 204–209.

[11] M.H. Habibi, I.A. Farsani, Enhanced photocatalytic degradation of C.I. Reactive Orange 86 in aqueous environment using nanostructure $Zn_{1-x}Co_xO$ composite thin film coated on glass, Desalin. Water Treat. 22 (2010) 204–210.

[12] D. Barreca, A. Gasparotto, C. Maccato, E. Tondello, U.L. Štangar, S.R. Patil, Photoinduced superhydrophilicity and photocatalytic properties of ZnO nanoplatelets, Surf. Coat. Technol. 203 (2009) 2041–2045.

[13] K.H. Hu, Z. Liu, F. Huang, X.G. Hu, C.L. Han, Synthesis and photocatalytic properties of nano-MoS_2/kaolin composite, Chem. Eng. J. 162 (2010) 836–843.

[14] U.G. Akpan, B.H. Hameed, Solar degradation of an azo dye, acid red 1, by Ca–Ce–W–TiO_2 composite catalyst, Chem. Eng. J. 169 (2011) 91–99.

[15] H. Xu, H. Li, G. sun, Xia, C. Wu, Z. Ye, Q. Zhang, Photocatalytic activity of La_2O_3-modified silver vanadates catalyst for Rhodamine B dye degradation under visible light irradiation, Chem. Eng. J. 160 (2010) 33–41.

[16] S. Adishkumara, S. Kanmani, Treatment of phenolic wastewaters in single baffle reactor by Solar/TiO_2/H_2O_2 process, Desalin. Water Treat. 24 (2010) 67–73.

[17] S.R. Patil, U.L. Štangar, S. Gross, U. Schubert, Super-hydrophilic and photocatalytic properties of Ag–TiO_2 thin film prepared by sol-gel technique, J. Adv. Oxid. Technol. 11(2) (2008) 327–337.

[18] U.G. Akpan, B.H. Hameed, Enhancement of the photocatalytic activity of TiO_2 by doping it with calcium ions, J. Colloid Interface Sci. 357 (2011) 168–178.

[19] E.G.L. Oliveira, J.J. Rodrigues Jr., H.P. de Oliveira, Influence of surfactant on the fast photodegradation of rhodamine B induced by TiO_2 dispersions in aqueous solution, Chem. Eng. J. 172 (2011) 96–101.

[20] D.C. Hurum, A.G. Agrios, K.A. Gray, Explaining the enhanced photocatalytic activity of degussa P25 mixed-phase TiO_2 using EPR, J. Phys. Chem. B107 (2003) 4545–4549.

[21] R. Scotti, I.R. Bellobono, C. Canevali, C. Cannas, M. Catti, M. D. Arienzo, A. Musinu, S. Polizzi, M. Sommariva, A. Testino, F. Morazzoni, Sol gel pure and mixed-phase titanium dioxide for photocatalytic purposes: Relations between phase composition, catalytic activity, and charge-trapped sites, Chem. Mater. 20 (2008) 4051–4061.

[22] N. Bouanimba, R. Zouaghi, N. Laid, T. Sehili, Factors influencing the photocatalytic decolorization of bromophenol blue in aqueous solution with different types of TiO_2 as photocatalysts, Desalination 275 (2011) 224–230.

[23] R.J. Wu, C.C. Chen, C.S. Lu, P.Y. Hsu, M.H. Chen, Phorate degradation by TiO_2 photocatalysis: Parameter and reaction pathway investigations, Desalination 250 (2010) 869–875.

[24] L. Gomathi Devi, K. Mohan Reddy, Photocatalytic performance of silver TiO_2: Role of electronic energy levels, Appl. Surf. Sci. 257 (2011) 6821–6828.

[25] Y. Chen, D.D. Dionysiou, Bimodal mesoporous TiO_2–P25 composite thick films with high photocatalytic activity and improved structural integrity, Appl. Catal. B: Environ. 80 (2008) 147–155.

[26] C.K. Jyothi, K.B. Jaimy, S. Ghosh, S. Sankar, V.S. Smitha, K.G. K. Warrier, Titania–lanthanum phosphate photoactive and hydrophobic new generation catalyst, J. Solid State Chem. 184 (2011) 1867–1874.

[27] K.S.W. Sing, D.H. Everett, R.A.W. Haul, L. Moscou, R.A. Pierotti, J. Rouquerol, T. Siemieniewska, IUPAC, reporting physisorption data for gas/solid systems with special reference to the determination of surface area and porosity, Pure Appl. Chem. 57(4) (1985) 603–619.

[28] M. Ye, Z. Chen, W. Wang, J. Shen, J. Ma, Hydrothermal synthesis of TiO_2 hollow microspheres for the photocatalytic degradation of 4-chloronitrobenzene, J. Hazard. Mater. 184 (2010) 612–619.

[29] O. Carp, C.L. Huisman, A. Reller, Photoinduced reactivity of titanium dioxide, Prog. Solid State Chem. 32 (2004) 33–177.

[30] K. Mogyorosi, J. Nemeth, I. Dekany, J.H. Fendler, Preparation, characterization and photocatalytic properties of layered silicates supported TiO_2 and ZnO nanoparticles, Prog. Colloid Polym. Sci. 117 (2001) 88–93.

[31] Z. Zhang, C.C. Wang, R. Zakaria, J.Y. Ying, Role of particle size in nanocrystalline TiO_2-based photocatalysts, J. Phys. Chem. B 102 (1998) 10871–10878.

[32] S. Rabindranathan, S. Devipriya, S. Yesodharan, Photocatalytic degradation of phosphamidon on semiconductor oxides, J. Hazard. Mater. B 102 (2003) 217–229.

[33] S.K. Kansal, M. Singh, D. Sud, Studies on photodegradation of two commercial dyes in aqueous phase using different photocatalysts, J. Hazard. Mater. 141 (2007) 581–590.

[34] J.A. Anderson, Photocatalytic nitrate reduction over Au/TiO_2, Catal. Today 175 (2011) 316–321.